IEEE Photonics Journal
An IEEE Photonics Society Publication

Open Access
Invited Paper

Metamaterials in the Terahertz Regime

Volume 1, Number 2, August 2009

Withawat Withayachumnankul
Derek Abbott, Fellow, IEEE

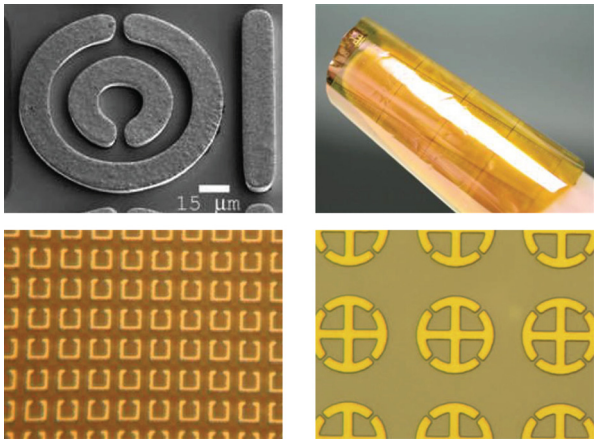

DOI: 10.1109/JPHOT.2009.2026288
1943-0655/$26.00 ©2009 IEEE

Metamaterials in the Terahertz Regime

Withawat Withayachumnankul[1,2] **and Derek Abbott,**[2] ***Fellow, IEEE***

(Invited Paper)

[1]Department of Information Engineering, Faculty of Engineering, King Mongkut's Institute of Technology Ladkrabang, Bangkok 10520, Thailand
[2]School of Electrical and Electronics Engineering, The University of Adelaide, Adelaide, SA 5005, Australia

DOI: 10.1109/JPHOT.2009.2026288
1943-0655/$26.00 ©2009 IEEE

Manuscript received May 20, 2009; revised June 17, 2009. First published Online June 26, 2009. Current version published July 29, 2009. Corresponding author: W. Withayachumnankul (e-mail: withawat@eleceng.adelaide.edu.au).

Abstract: Metamaterials are artificial composites that acquire their electromagnetic properties from embedded subwavelength metallic structures. In theory, the effective electromagnetic properties of metamaterials at any frequency can be engineered to take on arbitrary values, including those not appearing in nature. As a result, this new class of materials can dramatically add a degree of freedom to the control of electromagnetic waves. The emergence of metamaterials fortunately coincides with the intense emerging interest in terahertz radiation (T-rays), for which efficient forms of electromagnetic manipulation are sought. Considering the scarcity of naturally existing materials that can control terahertz, metamaterials become ideal substitutes that promise advances in terahertz research. Ultimately, terahertz metamaterials will lead to scientific and technological advantages in a number of areas. This article covers the principles of metamaterials and reviews the latest trends in terahertz metamaterial research from the fabrication and characterization to the implementation.

Index Terms: Metamaterials, THz optics.

1. Introduction

Metamaterials are fascinating new manmade materials that can manipulate beams of light in surprising ways. Their structure is basically composed of subwavelength metallic resonators held together in a dielectric. The electromagnetic properties of metamaterials are derived mainly from these resonating elements rather than from atoms or molecules as do conventional materials [1]. The term "metamaterial" coined by Walser [2] was originally defined as a 3-D periodic artificial composite producing a combination of two or more electromagnetic responses not found in nature. Nevertheless, some so-called metamaterial structures emerging later on did not exactly comply with this definition. Although currently there is no scientific consensus on what constitutes metamaterials, the common attributes that may be used to classify metamaterials are as follows [3]: i) The structure can be described by a set of effective homogeneous electromagnetic parameters; ii) the parameters are determined by the collective response of small conducting resonators; iii) the resonators are placed periodically therein; and iv) the ratio of the operating wavelength to lattice constant is of the order of ten or more. These attributes clearly distinguish metamaterials from other manmade wave-manipulating structures, such as photonic crystals [4], metallic hole arrays [5], [6], or frequency-selective surfaces [7].

Metamaterials can be engineered to have a wide range of electromagnetic characteristics at desired frequencies. This includes those characteristics not found in naturally occurring materials, and hence the name "meta," which implies "beyond" materials. In terms of the real electric permittivity and magnetic permeability, normal dielectrics typically occupy the domain where both quantities are positive. Negative values of the permittivity are attainable in nature through the radiation-plasma interaction, but the occurrence of this interaction is typically well beyond the infrared for those solid-state plasmas. Metamaterials, e.g., thin-wire lattices [8], can dilute the plasma cloud and shift the plasma frequency to a lower part of the spectrum, resulting in a negative permittivity at lower frequencies. In nature, negative values of permeability are rare and obtainable from magnetic resonances in ferromagnets at submicrowave frequencies. Metamaterials, such as split-ring resonators (SRRs) [9] and cut-wire pairs [10], can exhibit magnetic dipoles and negative permeability in response to magnetic waves up to the optical regime [11], [12]. Free tuning of electric and magnetic responses in metamaterials brings about the possibility to realize double-negative materials or negative-index materials (NIMs), in which the permittivity and permeability are less than zero at the same frequencies. Such materials have never been found in nature, because the negative bands of the permittivity and permeability are relatively narrow and stand well apart in the spectrum [13]. The first realization of NIMs exploits the combined operations of wires and SRRs to produce overlapping negative permittivity and permeability at microwave frequencies, respectively [14]. Due to this unusual behavior, NIMs have spurred a wide interest in metamaterials and become the center of metamaterial research aimed at operation in the visible frequency range [15]–[17].

By opening a new electromagnetic response regime, metamaterials offer immense opportunities in improving existing optical designs along with exploring unprecedented applications. Relevant research breakthroughs and visions proposed so far encompass: superlenses breaking the diffraction-limited image resolution [18]–[20], biosensors sensitive to small changes in the amount and response of a sample [21], magnetic wires retrofittable into existing MRI machines for a better magnetic coupling [22], invisibility cloaks for hiding an object from detection [23]–[26], and *illusion devices* replacing the object image with a different virtual image [27]. Because metamaterial research has recently emerged, fundamental studies, novel designs, and advanced applications of metamaterials have yet to be fully explored. It is believed that this novel research field will have great impact on both the physics and engineering disciplines.

This paper focuses on metamaterials that are designed to operate in the terahertz electromagnetic regime. Metamaterials are of particular interest in the terahertz regime, where most natural materials exhibit only weak electric and magnetic responses and hence cannot be utilized for controlling the radiation. The introduction of terahertz metamaterials is believed to be an important step that can further advance terahertz research and development. Based on this motivation, this paper thoroughly reviews principles, fabrication, characterization and potential applications of terahertz metamaterials that have emerged lately. But before looking into the current state of research on terahertz metamaterials, some background relating to metamaterials and terahertz radiation is discussed in Sections 2 and 3, respectively. Then, a few techniques currently employed to fabricate terahertz metamaterials are explained in Section 4. After that, fundamental studies of various types of terahertz metamaterials are reviewed thoroughly in Section 5. Section 6 discusses the possibilities of extending the usable frequency band of terahertz metamaterials that are fundamentally based on narrow-band resonances. State-of-the-art applications of terahertz metamaterials, such as absorbers, modulators, and molecular sensors, are surveyed in Sections 7–9. The paper concludes with a projection on the trend of terahertz metamaterial research in Section 10.

2. Theory of Metamaterials

Various types of subwavelength resonators, forming building blocks for metamaterials, have been introduced during the last decade, as for example: thin wires [8], [28], Swiss rolls [9], SRRs [9], electric SRRs (eSRRs) [29], [30], pairs of rods [10], [12], [31], pair of crosses [32], fishnets [17], [33], etc. Some of them are designed for either an electric or magnetic response, while the others display

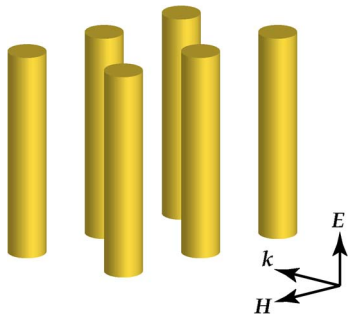

Fig. 1. Lattice of thin metallic wires. With an electric field parallel to the wires, the structure exhibits a Drude electric response with its plasma frequency governed by the geometry.

a negative refractive index. At the frequencies below infrared, the basic structures of thin wires and SRRs are sufficient to obtain the desired electromagnetic properties. Other advanced structures deriving their characteristics from wires and SRRs have been devised to sustain the desired properties at higher frequencies where metallic constituents lose their ideal conductivity and fabrication becomes too difficult for basic structures.

2.1. Lattice of Thin Wires

The electric response of natural conductive materials typically takes place at high frequencies, i.e., at the visible or UV band for metals. This is evident from the electric plasma frequency, ω_{ep}, which can be formulated as

$$\omega_{ep}^2 = \frac{ne^2}{\epsilon_0 m_{eff}} \tag{1}$$

where n is the electron density, e is the electron charge, ϵ_0 is the vacuum permittivity, and m_{eff} is the electron effective mass. For example, gold with an electron density of 5.9×10^{22} cm^{-3} has a plasma frequency located at approximately 138 nm or within the far UV range.

In order to achieve an electric response at a lower frequency range, e.g., in the microwave region, the plasma frequency must be modified. According to Equation (1) the plasma frequency can be reduced through changes in the electron density and effective mass. A metamaterial structure made of a lattice of thin metallic wires, similar to that shown in Fig. 1, is a workable solution [8]. In such a structure, the electron density n is diluted due to the sparseness of metal in a unit cell. Furthermore, the electron effective mass m_{eff} is intensified because of the apparent mutual inductance of the wires that exerts a force on the electrons. From the analysis, given that a is the lattice spacing and r is the wire radius, the plasma frequency of the structure now becomes [8], [28]

$$\omega_{ep}^2 = \frac{2\pi c_0^2}{a^2 \ln(a/r)} \tag{2}$$

where c_0 is the velocity of light in vacuum. It is clear that the plasma frequency of the structure can be manipulated merely through its dimensions, a and r. By assuming infinite wire length, the structure can be characterized by an effective permittivity that takes on a Drude model

$$\epsilon_{eff}(\omega) = 1 - \frac{\omega_{ep}^2}{\omega^2 + j\Gamma\omega} \tag{3}$$

where Γ is responsible for the propagation loss. At $\omega < \omega_{ep}$ the permittivity becomes negative.

2.2. SRRs

Magnetism is obtainable from nonmagnetic materials, provided that the materials can support current loops that bring about a magnetic dipole moment. By adopting this principle, SRRs, which

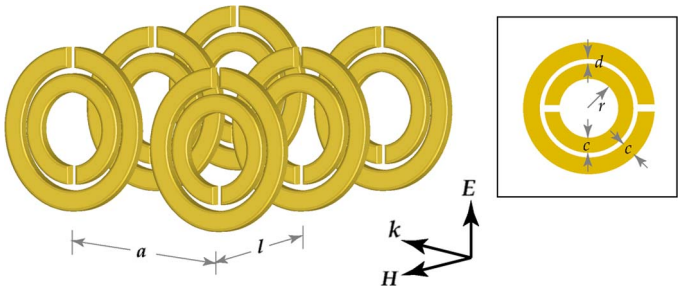

Fig. 2. Double SRRs. When excited by a magnetic field parallel to the SRR axis, the structure exhibits a Lorentzian resonance in the effective permeability. The electric field is parallel to the gap, and hence does not couple to the SRRs. The inset indicates the notation used for the geometrical features.

feature subwavelength conducting loops, can have a magnetic response under the proper alignment of the electromagnetic waves [9]. As shown in Fig. 2, a unit cell of the original double SRRs is basically composed of two concentric metallic rings with opposite splits or gaps. When the SRR is coupled to a magnetic field component oscillating in the axial direction, the ring establishes a current flow, which further builds a magnetic dipole parallel or antiparallel to the magnetic field. The loop inductance and gap capacitance are equivalent to an *LC* resonant circuit, causing a strong magnetic response at its resonance. The inner concentric ring contributes to the net capacitance of the double SRR and thus lowers the resonance frequency. Hence, this ring boosts up the ratio between the operating wavelength and lattice constant, making the SRRs appear more homogeneous to the electromagnetic excitation. In spite of this, the inner ring can be removed without a significant impact on the SRR's function while shifting the resonance frequency.

A metamaterial structure composed of periodically aligned SRRs under a magnetic excitation can be described by an effective magnetic permeability with a Lorentzian model [9]

$$\mu_{\text{eff}}(\omega) = 1 - \frac{F\omega^2}{\omega^2 - \omega_{\text{m0}}^2 + j\Gamma\omega} \tag{4}$$

where ω_{m0} is the magnetic resonance frequency, Γ represents the energy dissipation, and F is the fill factor of the SRR. The magnetic resonance frequency is related to the SRR's geometry through [9]

$$\omega_{\text{m0}}^2 = \frac{3lc_0^2}{\pi \ln\frac{2c}{d} r^3}. \tag{5}$$

The magnetic plasma frequency is where the permeability crosses zero and is given by

$$\omega_{\text{mp}}^2 = \omega_{\text{m0}}^2/(1 - F). \tag{6}$$

At frequencies lower than the resonance the SRRs have a positive response to the magnetic field, and between the resonance and plasma frequencies the response becomes negative. Therefore, the structure can support paramagnetism $(\mu_{\text{eff}} > 1)$ and diamagnetism $(\mu_{\text{eff}} < 1)$, including a negative permeability.

2.3. eSRRs

In the case that an electric field is parallel to the gap-bearing side, the SRRs in Fig. 2 can couple to the field, leading to an electric *LC* resonance at the same frequency as the magnetic *LC* resonance or ω_{m0} discussed above [34]. But the structure is in some sense bi-anisotropic, since the *LC*-mode electric excitation also causes a magnetic dipole in the axial direction [35]. This secondary effect may be unwanted where only an electric response is required. The symmetry of SRRs with respect to the electric field direction is introduced in order to suppress magnetic behavior and retain a pure electrical response [29]. These symmetric SRRs, dubbed eSRRs (also known as

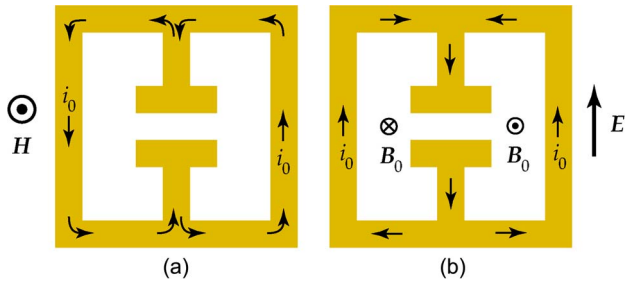

Fig. 3. eSRRs. (a) The external magnetic oscillation induces two identical looping currents that cancel each other, causing no magnetic coupling. (b) The external electric oscillation develops clockwise and anticlockwise currents that induce net zero magnetic flux density in the structure. The directions of polarizations, dipoles, and currents are at a time instance.

electric *LC* resonators), have neither magnetic nor magnetoelectric couplings. The schematics of the coupling modes are given in Fig. 3. Under uniform magnetic excitation, the circulating currents in the adjacent loops are equal and mutually nullified, yielding no magnetic response. For an electric excitation, opposite magnetic dipoles are induced in the adjacent loops, resulting in a net zero magnetic dipole, i.e., no magnetoelectric coupling.

In addition to the fundamental mode or *LC* resonance, higher modes of electric resonances, such as dipole or quadrupole, can be excited in eSRRs, but these resonances are no longer in the effective medium limit, i.e., the wavelength-to-lattice ratio becomes closer to unity. Therefore, these higher modes are less relevant to the operation of metamaterials.

2.4. Wires/SRRs Combination

In 1968 Veselago [36] raised a series of questions about a hypothetical material with simultaneous negative electric and magnetic responses—whether it is possible, how it interacts with the radiation, and where it can be found. Purely from the theoretical viewpoint he asserted that such a material can exist and does not violate any law of physics, and moreover it interacts with the electromagnetic wave in novel ways. Essentially, in a material with a permittivity and permeability being subzero, ***E*** and ***H*** form a left-handed vector set with respect to ***k***, i.e., the wave vector becomes negative. In contrast, the Poynting vector ***S***, indicating the propagation direction of wave energy, still forms a right-handed triplet with ***E*** and ***H***. Hence, the wavefront propagates backward in the medium, and is antiparallel with the direction of energy flow. Postulated by Veselago, this kind of medium, if realized, would exhibit a number of intriguing phenomena, including the reversed Doppler, reversed Cherenkov radiation, and negative refraction. Furthermore, he suggested that negative permittivity and permeability are most likely to occur in natural anisotropic substances, but none has been found to date. Note that the term "left-handed materials", inferred from the left-handed vector triplet, was adopted in early work, but this term is also used in the context of chirality and thus can be misleading. Consequently, to avoid confusion with chiral materials the terms *NIMs* or *double-negative materials* are currently preferred.

The idea of NIMs had remained theoretical for more than 30 years since its first introduction. The advent of metamaterials with tailored electric [8] and magnetic [9] responses pointed the way toward a possible implementation of NIMs by combining the two classes of metamaterials. The fill factors of metamaterials are so small that the mutual interaction between the two classes is minimized, and their original characteristics, namely the negative permittivity and permeability, are preserved [37]. The first NIM, realized by Smith *et al.* [14] in 2000, combines copper SRRs and thin wires, as shown in Fig. 4, to produce negative μ and ϵ in the microwave frequency band. A transmission measurement reveals a passband around 5 GHz, implying the presence of negative refractive index, since the negative permittivity or permeability alone will prohibit the propagation modes. The result was reproduced with similar experiments [38], [39] and with a refined numerical simulation [40].

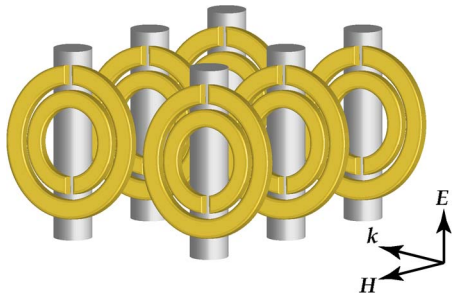

Fig. 4. NIM. A periodic array of SRRs interleaved with thin wires is oriented in the electromagnetic field such that the magnetic field is parallel to the SRR axis and the electric field is parallel to the wire axis. The wires and rings are responsible for electric and magnetic responses, respectively. At a narrow frequency band the permittivity and permeability are negative, resulting in the demonstration of negative refractive index.

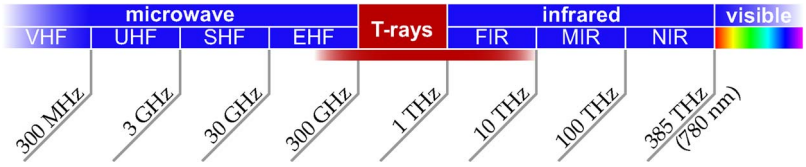

Fig. 5. Terahertz band and its neighboring designations. The terahertz (T-ray) band is loosely defined between 0.1 and 10 THz, the lower and upper parts of which overlap with the conventional designation of EHF microwave (millimeter wave) and far infrared, respectively.

3. Terahertz Spectrum

The current trend of metamaterial research involves designing and fabricating nanostructures that are capable of manipulating electromagnetic waves at the visible frequency regime [15], [16], [41], [42]. Although in theory metamaterial structures are physically scalable to fit a working spectral regime, approaching short wavelengths in the visible regime is challenging in terms of fabricating the required feature sizes [43]. In addition, at higher frequencies, metals begin to deviate from a perfect conductor and raise the issue of energy dissipation in metamaterials [44]. The latest efforts in metamaterial research will soon lead to optical nanostructures that are of primary importance to the fields of communication, microscopy, and defense. As significant as the optics, the terahertz spectrum represents another major research arena of metamaterials.

The terahertz (T-ray) regime is loosely defined between 0.1 and 10 THz, as indicated by the diagram in Fig. 5 [45], [46]. This spectral band, bridging the worlds of electronics and optics, has been relatively unexplored and is referred to as the *terahertz gap* because of accessibility difficulties. It is only recently that terahertz technology has been developed to the point where the frequencies can be generated, detected, and manipulated routinely with tabletop equipment. Amongst many techniques [47], terahertz time-domain spectroscopy (THz-TDS) [48] utilizing a femtosecond laser source is a potential candidate for generation and detection of broadband coherent terahertz radiation. The excitation of the emitter with ultrashort laser pulses results in a burst of subpicosecond pulses with frequencies spanning from a few hundred gigahertz to a few terahertz. At the detector, a coherent detection scheme is capable of resolving the amplitude and phase of a terahertz pulse with an adequate SNR.

Many distinctive properties are associated with terahertz frequencies. The radiation is nonionizing and hence favorable to applications seeking human exposure, e.g., medical diagnoses or security screening. A myriad of materials display unique absorption patterns in response to the terahertz waves, in accordance with their molecular rotational/vibrational modes [49]. These absorption spectra lend themselves to substance identification [50], [51]. Nonpolar, dry, and nonmetallic materials, such as fabrics, woods, cardboards, and plastics, are transparent to the radiation. Hence, weapons concealed beneath clothing or products contained in packages, for example, can be seen via a terahertz sensor [52]–[54]. Despite that, the applications of terahertz

largely remain laboratory based, pending improved performance in the areas of generation, control, and detection. Essentially, more terahertz components are demanded to support applications.

The terahertz spectrum represents a fascinating arena for metamaterial research in light of the fact that naturally occurring materials do not exhibit strong magnetic or electric responses between 1 and 3 THz [55]. Those conventional magnetic materials tend to have resonances at frequencies below the gigahertz range, while metals possess resonances at frequencies beyond the mid-infrared owing to phonon modes. Thus, in this sense, the *terahertz gap* not only defines a spectral region that has rarely been explored, but also a region where the electromagnetic responses of most natural materials diminish. These weak responses can be considered as another factor that hinders the progress of terahertz research so far. Because of their customizable characteristics, metamaterials can complete the missing link, and become versatile tools for future terahertz research and development. Ultimately, these metamaterials are expected to develop into terahertz-manipulating devices that outperform their predecessors, or moreover, which are not possible with conventional materials.

It is rather obvious that metamaterials can greatly propel terahertz technology. Vice versa, terahertz technology can advance our understanding of the fine interactions between metamaterials and electromagnetic waves in general. At frequency regimes beyond the terahertz band, the fabrication of metamaterials can be very challenging with present technologies. On the other hand, prevalent IC fabrication laboratories can realize prototypes of planar terahertz metamaterials with ease. The information obtainable from terahertz metamaterials can be beneficial to the study of optical metamaterials, as terahertz radiation maintains quasi-optical behaviors. Additionally, terahertz measurement systems, in particular THz-TDS, offer a great deal of flexibility unavailable from other spectroscopic modalities. The broadband amplitude and phase detection together with the flexible configuration of the system permits the full characterization of metamaterial properties. For these reasons, the terahertz frequency regime is very attractive for experimental demonstrations of metamaterial prototypes.

4. Fabrication of Terahertz Metamaterials

As mentioned earlier, although the scalability in theory suggests a direct adoption of certain metamaterial designs for operating at any frequency band across the spectrum, in reality, there exist several implications that may affect the performance of metamaterials. Although not directly related to the responses of metamaterials, the constituents, i.e., metals and dielectrics, play a major role in the energy dissipation [56]. At an operating frequency range, metals and dielectrics need to be highly conductive and insulating, respectively, to obtain the strongest electromagnetic responses from metamaterials. For any frequency band, suitable fabrication processes must be sought to satisfy the requirements of, for instance, 3-D operation, low cost, and mass production.

Current IC fabrication technologies are very suitable for producing planar terahertz metamaterials—also known as *metasurfaces* or *metafilms*—described by a single metallic layer deposited on an insulating substrate or embedded in a matrix with the smallest geometric features of a few micrometers. These technologies account for most of the terahertz metamaterials reported so far (see Fig. 6 for example). There is little restriction on the types of metals and dielectrics that can be used in the fabrication, and even thin polymer films, which are flexible and highly transparent to terahertz, can be employed for the substrate [58], [60]. Semi-insulating substrates may be locally doped so that at certain locations the conductivity can be altered by an external stimulus for enhanced functionality of metamaterials [61], [62]. The small size of metamaterials fabricated on a large wafer leads to the economy of scale, as a single wafer can accommodate many metamaterial devices. Despite these advantages, metasurfaces raise the issue of magnetic coupling; incident plane waves normal to a metasurface cannot induce magnetism that requires loop-like metallic resonators lying in the direction of propagation. This issue may be resolved by using an oblique angle of incidence that allows a component of the magnetic wave to couple to an array of SRRs [59], [63], [64]. With the wave incident at an angle to the surface, planar wires/SRRs fabricated on several glass plates [65] or SU-8 resist [66] are able to exhibit negative refractive

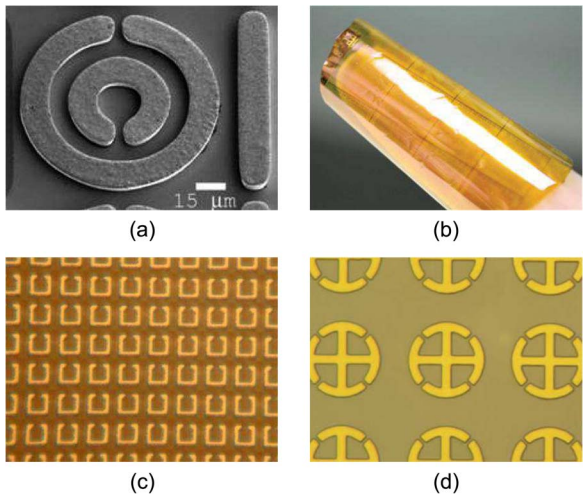

Fig. 6. Various terahertz metamaterials produced using lithography & deposition processes. These metamaterial patterns with feature sizes of the order of micrometers exhibit strong tailored electromagnetic responses at terahertz frequencies. (a) NIM from a ring-wire structure. After [57]. (b) Free-standing polyimide substrate embossed by micro SRRs. After [58]. (c) Array of SRRs fabricated in polyimide. After [59]. (d) Polarization-invariant eSRRs deposited on GaAs. After [30]. Note that each image uses a different scale.

index. A more advanced design of a double-layer cross-wire structure embedded in a thin film of benzocyclobutene (BCB) can act as a NIM in response to the terahertz radiation incident normal to the surface [67].

Although the aforementioned metasurfaces, manufactured from ordinary IC production lines, can sufficiently demonstrate customizable terahertz responses, the structures are highly anisotropic and lacking of a 3-D distribution. Many metamaterial applications that rely on the advanced concept of transformation optics [23], [68], such as hyperlenses [20] or invisibility cloaks [24], necessitate a full control of the permittivity and permeability in three axes over a defined volume. In the microwave regime, metamaterials with a lattice constant of the order of millimeters can be readily assembled into 3-D units to satisfy such the requirement [69], [70]. Nevertheless, at terahertz and shorter wavelengths, achieving fully 3-D-functioning structures is challenging. Through the removal of a rigid substrate, a fabricated planar metamaterial may extend its functions into 2-D, as for example, flexible metasurfaces [58] and free-standing S-strings [71]. Besides more complex fabrication methods have been introduced to produce special 3-D structures. For instance, stereolithography (3-D printing) is used to realize free-standing pillars for negative permittivity [72], and inclined X-ray lithography is proposed to develop nonplanar SRRs on a substrate [66], [73]. Due to the complication of these techniques, 3-D terahertz metamaterials are not widespread. In order to facilitate progress in advanced metamaterial applications, new manufacturing processes, along with novel designs of metamaterials, have yet to be explored.

5. Fundamental Studies of Terahertz Metamaterials

Since the first realization of terahertz metamaterials in 2004 [63], nearly all metamaterial schemes, exhibiting either electric, magnetic, or both responses, have been scaled to and studied at the terahertz regime. Most studies involve standard characterizations for effective medium properties, e.g., the transmission, permittivity, and permeability, using either THz-TDS or FTIR spectroscopy. In addition, in-depth studies on the fine interaction between the terahertz radiation and metamaterials have increasingly gained interest because of the progress in terahertz near-field imaging.

5.1. Electric Responses

Electric responses at terahertz frequencies are mostly demonstrated with planar SRRs, along with their variants, as illustrated in Fig. 7. Typically, their electrical coupling modes are excited by

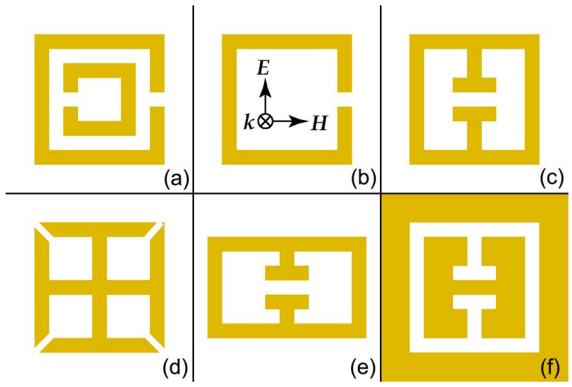

Fig. 7. Some SRR variants studied at terahertz frequencies. The variants shown here are (a) double SRR, (b) single SRR, (c) eSRR, (d) four-fold rotational-symmetry eSRR, (e) rectangular eSRR, and (f) complementary eSRR. The common field orientation is indicated for all structures, excepting for the complementary eSRR that requires the in-plane 90° field rotation. The illustrations are not to scale.

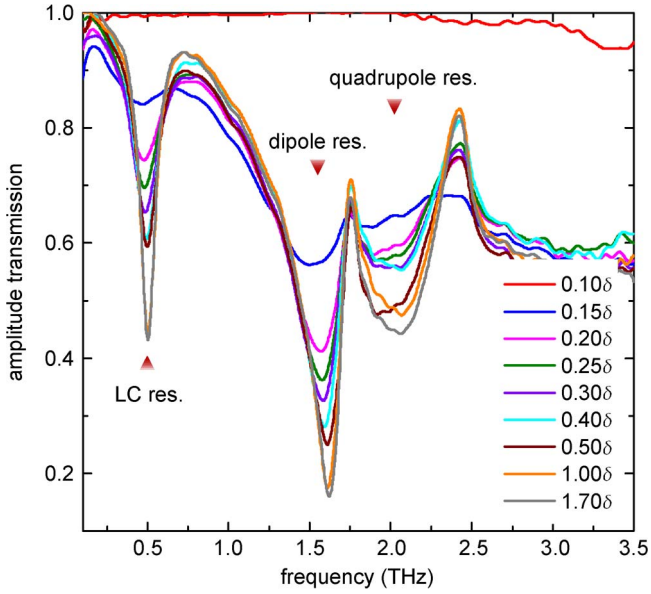

Fig. 8. Resonance as a function of SRR thickness. The SRR type and field orientation are according to Fig. 7(a). Multiple modes of resonances are indicated. In this experiment, the metal used to form the SRRs is lead (Pb) with a skin depth δ of 336 nm at 0.5 THz. After [76].

using wave propagation perpendicular to the SRR plane. In a study of double SRRs [see Fig. 7(a)] at terahertz frequencies, the effects of the shape (either square or circular), polarization, substrate, and lattice constant on the resonance properties are observed. For the polarization parallel to the gap-bearing side, *LC* and dipole resonances are present, but the *LC* resonance disappears in the other polarization [74]. The lattice constant largely affects the dipole and not the *LC* resonances, while a higher dielectric constant of the substrate causes a redshift to every resonance [74]. As indicated by another study on terahertz metamaterials, the gap orientation among single SRRs [see Fig. 7(b)] has a remarkable impact on the dipole resonance due to the inter-ring coupling nature [75]. The thickness of SRRs is also a topic of interest in terahertz spectroscopy. Metallic SRRs with a sub-skin-depth thickness have a large resistance such that the characteristic resonances are damped and eventually become extinct [76]. The evolution of the SRRs' resonances at terahertz frequencies with respect to the metal thickness is given in Fig. 8.

A number of eSRRs are designed to resonate in the terahertz regime [30], [77]–[80]. The standard eSRRs [see Fig. 7(c)] basically suppress a magnetic response in favor of a pure electric

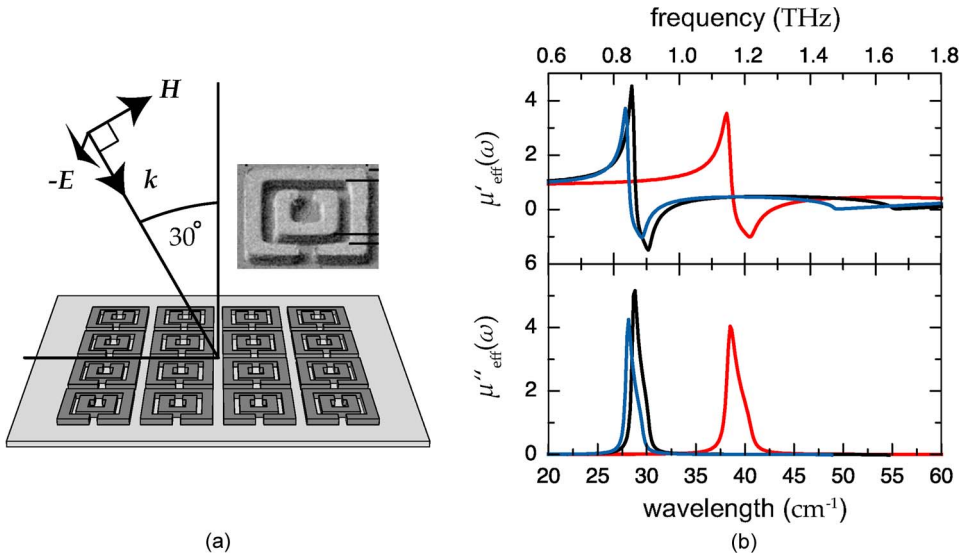

Fig. 9. Magnetically coupled SRRs. (a) The terahertz radiation incident on the SRRs at 30° from the normal. The configuration enables a magnetic field component to couple to SRRs, but prohibiting an electric *LC* coupling. (b) The complex magnetic permeabilities of the structures simulated by using different geometries. After [63].

response, and the four-fold rotational-symmetry eSRRs [see Fig. 7(d)] are not sensitive to polarization [30]. The number and position of capacitive gaps present in eSRRs is shown to affect the position/linewidth of the *LC* resonance [77]. Rectangular eSRRs [see Fig. 7(e)], as opposed to square eSRRs, allow tuning of the dipole resonance frequency. Provided that the area encircled by an SRR is fixed, the *LC* resonance frequency is kept constant, while the dipole resonance can be shifted to a higher frequency by shortening the SRR side that is parallel to an electric field [77], [78]. This tuning scheme can prevent the *LC*-dipole coupling that causes resonance reshaping. Terahertz eSRRs and their complements [see Fig. 7(f)] demonstrate consistency with Babinet's principle in that they display a transmission reversal, i.e., the transmission dips in eSRRs are manifested as the transmission peaks in complementary eSRRs [79], [80]. The complex permittivity profiles show that in the complementary eSRRs, a Drude response takes place as a result of a large metallic plane.

5.2. Magnetic Responses

In addition to electric responses, artificial magnetic responses are also demonstrated at terahertz wavelengths. The first realization employs an array of planar double SRRs, shown in Fig. 9, to produce a strong magnetism around 1 THz in response to obliquely incident waves [63]. This artificial magnetic material exhibits resonant strength an order of magnitude larger than that of natural magnetic substances. A similar measurement with single SRRs demonstrates a magnetic resonance at 6 THz [59]. Another structure containing multilayers of planar SRRs encapsulated in a polyimide film is magnetically active at 6 THz following an electric excitation on a gap-bearing side with the propagation direction normal to the SRR plane [81]. In this case, no magnetic response is actually observed at the far field, i.e., $\mu_{\text{eff}} = 1$, because the incident magnetic field is completely in the SRR plane and perpendicular to the induced magnetic dipole moment. For magnetic metamaterials, extracting a full set of effective parameters, i.e., ϵ', ϵ'', μ', and μ'', requires both transmission and reflection measurements of the amplitude and phase spectra, which are usually hard to obtain. It is proposed that the transmission amplitudes measured at several oblique angles of incidence are adequate to the task [82]. The parameters are retrieved by fitting appropriate Fresnel models to the transmission data. The method is successfully verified with terahertz magnetic SRRs possessing a magnetic resonance at 1.1 THz.

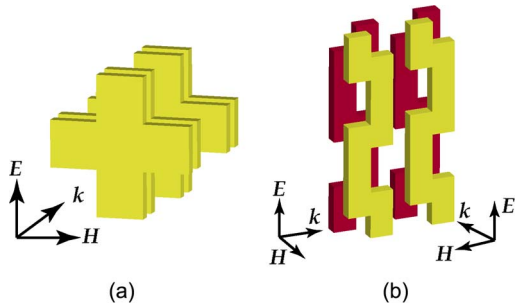

Fig. 10. Two different negative-index materials. (a) Two unit cells of crossbars display a negative index in response to the wave incident normal to the surface. (b) Bi-layer S-strings behave as a 2-D-isotropic NIM, owing to the presence of current loops in either direction of propagation.

5.3. Negative Refractive Index

Beyond purely electric or magnetic media, terahertz metamaterials investigated so far encompass NIMs that possess spectrally overlapping negative permittivity and permeability. The prototypes at terahertz wavelengths are not limited to the conventional wire-ring combination, but include advanced NIM structures, such as crossbars, S-strings, and chiral media. In one design, terahertz NIMs containing planar SRRs and wires fabricated on the same layer [see Fig. 6(a)] allow properly aligned electric and magnetic field components to resonate and support a passband at around 2 THz [57], [73] and 4.92 THz [66]. Another NIM structure involves double layers of metallic crossbars, as shown in Fig. 10(a). Each metallic bar is responsible for an electric dipole and negative permittivity, while the two metallic layers, in substitution of an SRR, are responsible for a magnetic dipole and negative permeability. The crossbars at the terahertz scale show a NIM band around 1 THz with a figure of merit up to 11 [67]. Obviously, the structure in Fig. 10(a) is polarization independent for the propagation direction normal to the cross plane, due to the orthogonal symmetry. By introducing a geometrical disparity into the perpendicular bars, the NIM bands for the two polarizations are no longer identical and the structure becomes birefringent [83]. S-shape resonators, as illustrated in Fig. 10(b), are scaled to function in the terahertz regime. The interplay between the strings permits antiparallel currents and magnetic resonances in two propagation directions. In an experiment with free-standing S-strings, the NIM bands appear at 2.2 and 1.9 THz for the normal and 90° angle of incidence, respectively [71]. Unlike other NIMs, chiral metamaterials emerge as a special class of NIMs that is not necessarily underpinned by simultaneous negative permittivity and permeability [84]. In a chiral material, the left-handed and right-handed circularly polarized waves travel with different phase velocities, and in the case of a strong chirality, the phase velocity of one circular polarization may become negative. The chiral effect is a result of the cross coupling between electric and magnetic dipoles, which can be artificially reproduced by using nonplanar resonators [85]. A terahertz chiral metamaterial produces a negative refractive index between 1.06–1.27 THz [85].

5.4. Near-Field Terahertz Imaging of Metamaterials

The experiments discussed earlier primarily observe the far-field responses of terahertz metamaterials with an assumption of their homogeneity. In fact, these far-field characteristics are caused by the collective responses of subwavelength inhomogeneous resonators. A closer observation into these microscopic interactions can be accomplished via terahertz near-field imaging [86], [87]. In one experiment, an aperture-based technique is used to directly observe the electric field distribution near a metasurface [86]. The measured in-plane electric fields can be further used to determine a change in out-of-plane magnetic fields through a Maxwell's equation. The reported configuration places the detector at only 30 μm away from the surface of double SRRs, resulting in the spatial resolution of 20 μm compared with the shortest operating wavelength of 750 μm (400 GHz). The measurable electromagnetic fields clearly depict the mechanism

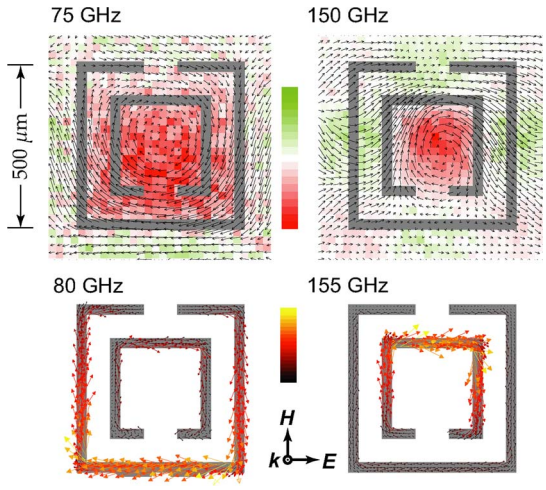

Fig. 11. Terahertz near-field imaging of double SRRs. (Top) The measured in-plane electric fields are shown in vectors at two frequencies, which are associated with the *LC* resonances of the outer and inner rings. The time derivative of the magnetic fields normal to the surface is shown as color coding. (Bottom) The simulated current densities coincide with the measurements. After [86].

underlying each mode of the far-field electric resonances. As an example in Fig. 11, at the near field, the electric fields encircling the rings are responsible for the far-field *LC* resonances at 75 and 150 GHz. Additionally, the information about field constructive/destructive interferences among neighboring resonators can describe variations in the resonance strengths. In another study, an apertureless terahertz microscopy with a resolution of 1 μm assists the interpretation of an ambiguous mode of resonance in eSRRs [87]. In this case, a near-field image presents a local contrast, as a result of the capacitive coupling between the measuring tip and the resonator. It is deduced from the measurements that the ambiguous resonance is caused by surface plasmons coupled to incident terahertz waves through the periodicity of the structure.

The knowledge acquired from terahertz metamaterials so far is beneficial to both terahertz and metamaterial technologies. Certainly, advanced terahertz devices will gain advantages from this material infrastructure. On the other hand, because metamaterials hold a scalable property, the acquired knowledge is fundamental to the improvement in metamaterial performance across the spectrum from microwave to infrared to visible light. Likewise, the information obtained from other frequency bands may be applied to terahertz metamaterials in the same manner.

6. Broadening the Bandwidth of Terahertz Metamaterials

The operation of ordinary metamaterials is confined within a narrow spectral range, since dispersive resonances are exploited to control the permittivity and permeability. This comes to a major hurdle for most applications that demand broadband operation. At various frequency bands, a number of solutions to the problem have been proposed, for example, multiresonance metamaterials [88]–[90] and passive [39], [64], [91], [92] or active [62], [93]–[97] resonance-tunable metamaterials.

At terahertz frequencies, the multiresonance approach has been realized with a few configurations. A straightforward configuration packs together two or more resonators with different geometries in a single unit cell. The number of resonance frequencies that the structure can display is determined by the number of different resonators. Terahertz metamaterials featuring either two or three planar eSRRs per unit cell are implemented using a checkerboard [88] or beehive [89] pattern, respectively, to maximize the fill factor [see Fig. 12(a) for the beehive metamaterial]. Multiresonance structures of this type unavoidably compromise the resonance strength owing to the sparseness of identical resonators and the counteraction between different resonators [88]. In the worst case, desired properties may be suppressed [98], [99]. The concept of a fractal that describes the self-similarity of a shape at different scales is an alternative. Metamaterials made of fractal H-shaped

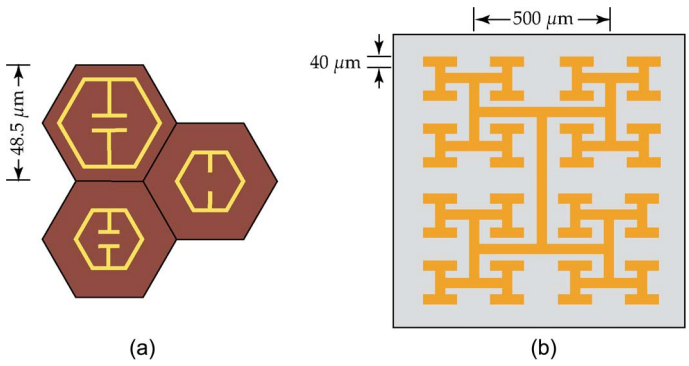

Fig. 12. Multiresonance metamaterials. (a) A unit cell of metamaterial containing a triplet of distinct eSRRs exhibits three distinct resonances. After [89]. (b) A H-type fractal metamaterial (6 levels shown here) displays several electric resonances corresponding to different wire lengths. After [90].

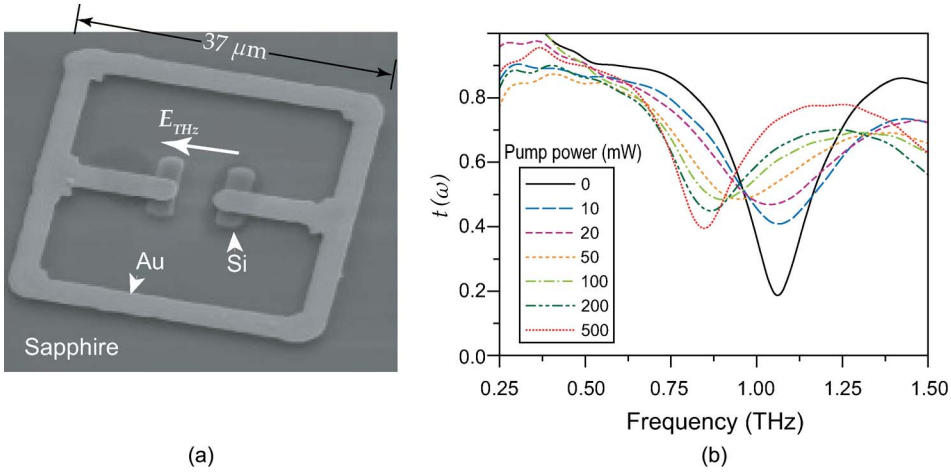

Fig. 13. Frequency-agile terahertz metamaterial. (a) A unit cell of eSRRs couples to an incident terahertz electric field. The small silicon plates positioned at the gap enhance the gap's capacitance upon a photoexcitation. (b) The corresponding transmission amplitudes indicate the resonance tunability following changes in the photoexcitation power. After [62].

metallic lines or slits, shown in Fig. 12(b), are able to display electric resonances at multiple terahertz frequencies [90]. Each fractal level contains a set of wires with a unique length that is responsible for an electric dipole resonance. However, in practice, fractal metamaterials cannot accommodate self-similar patterns at ever-finer scales.

Resonance tunability is a viable approach that permits relocating a resonance over a certain frequency range. This can be readily accomplished with an *LC* resonance by altering its *LC* constant through one of many possible ways. For a planar terahertz metamaterial that occupies a small area, its surface that is exposed to free space may be loaded with a dielectric of different amounts [64] or different types [92]. The loaded dielectric with a relative permittivity greater than one increases the resonators' capacitance and causes a redshift in the resonance. Although the tuning step can be continuous, on-the-fly tuning is not feasible.

Active resonance tuning allows a resonance to rapidly sweep over a continuous frequency range even during metamaterial operation. This approach is demonstrated in the microwave region with SRRs, whose resonances can be electrically tuned via variable capacitors shunting the resonators' gaps [93]–[95]. For shorter wavelengths, incorporating such a lumped circuit component into a metamaterial is unlikely, and thus alternatives must be sought. At terahertz wavelengths eSRRs are configured with intrinsic silicon plates deposited next to each gap, as shown in Fig. 13 [62]. An optical excitation generates free carriers in the plates, raising the gap capacitance. A redshift in the

LC resonance can then be observed within the terahertz band. The technique achieves an electric resonance tunability of 20%. Rather than controlling the gap capacitance, another configuration of tunable terahertz metamaterials relies on a change in the properties of a heavily doped semiconductor that forms SRRs [100]. An external magnetostatic field with an appropriate orientation can affect the complex permittivity of the semiconductor, resulting in a redshift of the SRRs' resonance. Simulation clearly depicts the dependence of the frequency shift on the magnitude of a magnetostatic field [100].

7. Substituting Conventional Terahertz Components With Metamaterials

Owing to their customizable electromagnetic properties, metamaterials have filled the terahertz gap where only a small number of natural materials can provide sufficiently useful characteristics. The consequences are immense in terms of potential terahertz devices. Discussed in this section, a variety of terahertz components based on terahertz metamaterials have been proposed. These include terahertz filters, perfect absorbers, quarter-wave plates, modulators, molecular sensors, and much more to come. Note that due to their broader impact, terahertz modulators and molecular sensors are presented in Sections 8 and 9.

The presence of either a negative permittivity or permeability alone in a metamaterial can be exploited to implement a frequency stopband, because in this region no propagation mode is permitted. As discussed in Section 2.1, a lattice of long metallic wires produces a negative permittivity below the plasma frequency, which can be positioned arbitrarily depending on the lattice geometry. A structure constructed from gold-coated polymer columns confirms the appearance of a stopband below the plasma frequency at 0.7 THz when an electric field is aligned parallel to the columns [72]. Since the coating thickness of gold is larger than its skin depth, the effect of the polymer columns can be ignored. Other types of filters can be implemented from metamaterials on a similar basis.

The impedance-matching capability and on-resonance absorption in metamaterials can be exploited for narrow-band terahertz absorbers. A structure comprising two electric and magnetic resonators in a unit cell is designed such that the permittivity/permeability pair results in impedance matching between the structure and free space in a narrow frequency band around 1.3 THz [101]. In addition, the high absorption inherited from the resonance activity is also positioned at 1.3 THz in order to lessen the overall transmittivity. As a result, terahertz waves of these frequencies incident on the absorber undergoes neither reflection nor transmission, i.e., they are almost perfectly absorbed. This metamaterial absorber is ideal for using in thermal detectors.

Because of their strong birefringence, certain metamaterial designs can be utilized for quarter-wave plates, which are able to transform linearly polarized waves into circularly polarized waves and vice versa. Two orthogonal fields of the same frequency can experience 90° phase shift in a metamaterial wave plate through the dispersive responses of independent horizontal and vertical dipole resonances. In an experiment, an array of rectangular eSRRs fabricated on a thin film of polyimide, with the total thickness of 20 μm, produces almost perfect circular polarization at 0.64 THz [102]. As opposed to an equivalent meanderline polarizer [103], the eSRR plate is almost four times thinner, but operates at a slightly narrower frequency band [102]. Another terahertz quarter-wave plate operating at 0.64 THz exploits pairs of asymmetric crossbars that exhibit ordinary and extraordinary *negative* refractive indices with a maximum index difference of 0.727 [83].

In many cases, it is proven that metamaterial-based terahertz devices outperform their conventional counterparts. But due to the resonant nature of metamaterials, their functions are restricted to a narrow spectral band that may be ideal for applications employing CW terahertz sources/detectors. Incorporating frequency tunability or other band-extension schemes, as discussed in Section 6, would add a degree of usefulness to the devices.

8. Terahertz Modulators

As the performance of existing terahertz switches and modulators proves to be impractical, metamaterials offer an alternative in dynamic manipulation of terahertz waves. With some modification to metamaterials, their resonances can be turned on/off via an external stimulus,

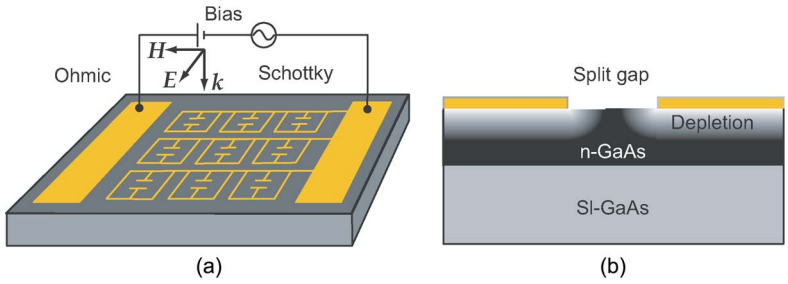

Fig. 14. Electrically controlled terahertz modulator. (a) A layout showing an array of planar eSRRs, biasing pads, external electric circuit, and exciting terahertz field. The eSRRs form a Schottky contact with the substrate. (b) A cutaway view reveals a build-up of the depletion region underneath the metal as a result of the reversely biased Schottky junction. After [61].

leading to a modulation depth in the transmission amplitude. This concept is implemented with a narrow-band terahertz modulator [104]. In that work, copper SRRs are fabricated on a high-resistivity GaAs substrate, and the terahertz wave is coupled to an electric resonance mode of SRRs. Under the influence of an optical excitation, the substrate becomes conductive via photo-induced free carriers, shorting the SRR gaps and thus eliminating the resonance absorption. This implies that the modulator is in its on state at resonance. In the absence of an optical excitation, the resonance is restored, leading to the off state. A faster terahertz modulator replaces the substrate with a ErAs/GaAs supperlattice with a faster carrier recombination, resulting in a switching recovery time of picoseconds or shorter [105].

In another type of terahertz modulator the on/off state is controllable via an external electric bias [61]. The structure, shown in Fig. 14, is constructed from gold eSRRs deposited on a thin *n*-type GaAs layer, which is grown on an intrinsic GaAs substrate. A group of conductive wires connects these resonators to a voltage source. In the absence of an external voltage, no resonance is observed as the *n*-type substrate electrically bridges the resonator gaps. Because the gold resonators form a Schottky contact with the substrate, a negative bias can deplete free electrons from the gap region, leading to a resonance response. The device is capable of modulating narrow-band terahertz at a kilohertz cycle, limited only by the stray capacitance. An improved version with a reduction in the RC time constant through layout redesigning is able to modulate terahertz waves at over 2 MHz [106].

It is shown that a terahertz modulator having a similar design to that in Fig. 14 is also able to modulate the terahertz phase [107]. Upon the application of an external voltage, changes can be observed in the transmission amplitude and phase at the resonance peak (0.81 THz) and wing (0.89 THz), respectively. The phase change achieves the modulation depth of 0.56 radian with a fixed insertion loss. Although the device operates at a narrow band, the combination of amplitude and phase modulations through the Kramers–Krönig relation allows a wideband modulation between 0.8 and 1.7 THz.

Compared to existing terahertz modulators, this new class of terahertz modulators constructed from metamaterials can demonstrate a promising performance, albeit principally confined to a narrow frequency band. An improvement to these devices is indeed viable. In the future, metamaterial-based terahertz modulators may become a significant component in emerging terahertz communications [108].

9. Molecular Sensing With Metamaterials

Fundamentally, terahertz radiation leads to a wide range of significant physical phenomena at the molecular level. In general, bulk dielectric relaxations and intermolecular motions occur in this frequency range [109]. Intermolecular hydrogen bonds in crystalline solids resonate at terahertz frequencies, causing distinctive absorption features [51]. Critical frequencies for Debye relaxation processes in liquids fall into the terahertz regime [109]. Pure rotational transitions can be observed when polar gases are stimulated by terahertz radiation [110]. Therefore, with these physical interactions involved, this frequency range is very attractive for the application of molecular sensing.

The sensing capability in the terahertz regime is augmented by the exceptional behaviors of metamaterials, particularly SRRs and eSRRs, which feature high-Q resonances and highly localized electric field concentration. A sharp resonance is necessary for sensing a small change in the sample dielectric constant, while a high field concentration minimizes the amount of sample required. An asymmetric SRR is designed to achieve both effects at terahertz frequencies [21]. A numerical study shows that once excited by an electric field the resonator exhibits dual resonances due to the coupling between two arcs with different lengths. The resonance shifts considerably after loading a sample onto the surface as a result of a change in the gap capacitance. An improved version of the asymmetric SRR utilizes a broken rectangular loop with sharp tips at its arms [111]. This rectangular design reduces the overall size of the structure, and the sharp tips result in a higher electric field confinement. In another experiment, magnetically activated SRRs operating at terahertz frequencies also indicate a possibility of molecular sensing through resonance shifting upon dielectric loading [64]. In addition to the plausible sensing capability, SRRs may prove viable for investigating the nonlinear response of a sample through their intense electric field concentration at the gap with no requirement for a powerful terahertz source.

10. Looking Into the Future

Not long after the first realization of metamaterials, these novel fascinating structures have already been developed into a number of practical terahertz devices, including filters, absorbers, switches, modulators, sensors, among other components, with their capabilities competitive to existing components. These developments have been assisted by intensive research into metamaterial-terahertz interactions, the advancement of metamaterial designs, and the prevalence of fabrication facilities. Above all, a shortage of strong terahertz characteristics in natural materials has provided a great impetus driving the research area of terahertz metamaterials.

Beyond replacing traditional components, metamaterials offer a new range of devices that exhibit unusual effects following their extreme electromagnetic properties. As an example, superlenses, which are able to amplify evanescent waves via exploitation of negative refractive index, have become a flagship application of metamaterials that attracts much interest in the radio [112], microwave [113]–[115], and optical [20], [116], [117] regimes. The implementation of these exotic lenses in the terahertz regime may advance terahertz sensing at the molecular level. But surprisingly, superlenses, as well as other devices based on extreme parameters, have not yet received much attention in this frequency regime.

We foresee that the development of terahertz metamaterials would benefit from the growing field of transformation optics [23], [68], which promises an arbitrary manipulation of electromagnetic waves. Currently metamaterials are limited by designs and fabrication techniques. Full control of electromagnetic parameters by future 3-D structures will certainly open up a whole new story of terahertz applications.

In conclusion, metamaterial research is a recent breakthrough that breaks the limited electromagnetic behavior of naturally occurring materials. Further research will alleviate the reliance on naturally occurring materials, by offering a wider range of customizable characteristics from artificial structures. This leads to a number of opportunities in developing new devices, for terahertz applications, where the use of existing materials lack strong electromagnetic interactions. The rapid development of terahertz metamaterials will propel the advance in terahertz applications. We can envision applications of terahertz metamaterials in the areas of astronomy, biochemistry, medicine, security, and communication in the near future.

References

[1] J. B. Pendry, "Metamaterials in the sunshine," *Nat. Mater.*, vol. 5, no. 8, pp. 599–600, Aug. 2006.
[2] R. M. Walser, "Electromagnetic metamaterials," in *Proc. SPIE—Complex Mediums II: Beyond Linear Isotropic Dielectrics*, 2001, vol. 4467, pp. 1–15.
[3] D. R. Smith and J. B. Pendry, "Homogenization of metamaterials by field averaging," *J. Opt. Soc. Amer. B, Opt. Phys.*, vol. 23, no. 3, pp. 391–403, Mar. 2006.

[4] E. Yablonovitch, "Photonic band-gap structures," *J. Opt. Soc. Amer. B, Opt. Phys.*, vol. 10, no. 2, pp. 283–295, Feb. 1993.
[5] T. W. Ebbesen, H. J. Lezec, H. F. Ghaemi, T. Thio, and P. A. Wolff, "Extraordinary optical transmission through sub-wavelength hole arrays," *Nature*, vol. 391, no. 6668, pp. 667–669, Feb. 1998.
[6] C. Genet and T. W. Ebbesen, "Light in tiny holes," *Nature*, vol. 445, no. 7123, pp. 39–46, Jan. 2007.
[7] R. Mittra, C. H. Chan, and T. Cwik, "Techniques for analyzing frequency selective surfaces—A review," *Proc. IEEE*, vol. 76, no. 12, pp. 1593–1615, Dec. 1988.
[8] J. B. Pendry, A. J. Holden, W. J. Stewart, and I. Youngs, "Extremely low frequency plasmons in metallic mesostructures," *Phys. Rev. Lett.*, vol. 76, no. 25, pp. 4773–4776, Jun. 1996.
[9] J. B. Pendry, A. J. Holden, D. J. Robbins, and W. J. Stewart, "Magnetism from conductors and enhanced nonlinear phenomena," *IEEE Trans. Microw. Theory Tech.*, vol. 47, no. 11, pp. 2075–2084, Nov. 1999.
[10] D. A. Powell, I. V. Shadrivov, and Y. S. Kivshar, "Cut-wire-pair structures as two-dimensional magnetic metamaterials," *Opt. Lett.*, vol. 16, no. 19, pp. 15 185–15 190, Sep. 2008.
[11] C. Enkrich, M. Wegener, S. Linden, S. Burger, L. Zschiedrich, F. Schmidt, J. F. Zhou, T. Koschny, and C. M. Soukoulis, "Magnetic metamaterials at telecommunication and visible frequencies," *Phys. Rev. Lett.*, vol. 95, no. 20, pp. 203 901-1–203 901-4, Nov. 2005.
[12] G. Dolling, C. Enkrich, M. Wegener, J. F. Zhou, C. M. Soukoulis, and S. Linden, "Cut-wire pairs and plate pairs as magnetic atoms for optical metamaterials," *Opt. Lett.*, vol. 30, no. 23, pp. 3198–3200, Dec. 2005.
[13] J. B. Pendry and D. R. Smith, "Reversing light with negative refraction," *Phys. Today*, vol. 57, no. 6, pp. 37–43, Jun. 2004.
[14] D. R. Smith, W. J. Padilla, D. C. Vier, S. C. Nemat-Nasser, and S. Schultz, "Composite medium with simultaneously negative permeability and permittivity," *Phys. Rev. Lett.*, vol. 84, no. 18, pp. 4184–4187, May 2000.
[15] V. Shalaev, "Optical negative-index metamaterials," *Nat. Photon.*, vol. 1, pp. 41–48, 2007.
[16] C. M. Soukoulis, S. Linden, and M. Wegener, "Negative refractive index at optical wavelengths," *Science*, vol. 315, no. 5808, pp. 47–49, Jan. 2007.
[17] G. Dolling, M. Wegener, C. M. Soukoulis, and S. Linden, "Negative-index metamaterial at 780 nm wavelength," *Opt. Lett.*, vol. 32, no. 1, pp. 53–55, Jan. 2007.
[18] J. B. Pendry, "Negative refraction makes a perfect lens," *Phys. Rev. Lett.*, vol. 85, no. 18, pp. 3966–3969, Oct. 2000.
[19] J. B. Pendry and D. R. Smith, "The quest for the superlens," *Sci. Amer.*, vol. 295, no. 1, pp. 60–67, Jul. 2006.
[20] X. Zhang and Z. Liu, "Superlenses to overcome the diffraction limit," *Nat. Mater.*, vol. 7, no. 6, pp. 435–441, 2008.
[21] C. Debus and P. H. Bolivar, "Frequency selective surfaces for high sensitivity terahertz sensing," *Appl. Phys. Lett.*, vol. 91, no. 18, pp. 184 102-1–184 102-3, Oct. 2007.
[22] M. C. K. Wiltshire, J. B. Pendry, I. R. Young, D. J. Larkman, D. J. Gilderdale, and J. V. Hajnal, "Microstructured magnetic materials for RF flux guides in magnetic resonance imaging," *Science*, vol. 291, no. 5505, pp. 849–851, Feb. 2001.
[23] J. B. Pendry, D. Schurig, and D. R. Smith, "Controlling electromagnetic fields," *Science*, vol. 312, no. 5781, pp. 1780–1782, Jun. 2006.
[24] D. Schurig, J. J. Mock, B. J. Justice, S. A. Cummer, J. B. Pendry, A. F. Starr, and D. R. Smith, "Metamaterial electromagnetic cloak at microwave frequencies," *Science*, vol. 314, no. 5801, pp. 977–980, Nov. 2006.
[25] N. A. Zharova, I. V. Shadrivov, and Y. S. Kivshar, "Inside-out electromagnetic cloaking," *Opt. Express*, vol. 16, no. 7, pp. 4615–4620, Mar. 2008.
[26] R. Liu, C. Ji, J. J. Mock, J. Y. Chin, T. J. Cui, and D. R. Smith, "Broadband ground-plane cloak," *Science*, vol. 323, no. 5912, pp. 366–369, Jan. 2009.
[27] Y. Lai, J. Ng, H. Chen, D. Han, J. Xiao, Z.-Q. Zhang, and C. T. Chan, "Illusion optics: The optical transformation of an object into another object," *Phys. Rev. Letts.*, vol. 102, no. 25, pp. 253 902-1–253 902-4, Jun. 2009.
[28] J. B. Pendry, A. J. Holden, D. J. Robbins, and W. J. Stewart, "Low frequency plasmons in thin-wire structures," *J. Phys., Condens. Matter*, vol. 10, no. 22, pp. 4785–4809, Jun. 1998.
[29] D. Schurig, J. J. Mock, and D. R. Smith, "Electric-field-coupled resonators for negative permittivity metamaterials," *Appl. Phys. Lett.*, vol. 88, no. 4, pp. 041109-1–041109-3, Jan. 2006.
[30] W. J. Padilla, M. T. Aronsson, C. Highstrete, M. Lee, A. J. Taylor, and R. D. Averitt, "Electrically resonant terahertz metamaterials: Theoretical and experimental investigations," *Phys. Rev. B, Condens. Matter*, vol. 75, no. 4, pp. 041102-1–041102-4, Jan. 2007.
[31] V. Shalaev, W. Cai, U. Chettiar, H. Yuan, A. Sarychev, V. Drachev, and A. Kildishev, "Negative index of refraction in optical metamaterials," *Opt. Lett.*, vol. 30, no. 24, pp. 3356–3358, Dec. 2005.
[32] C. Imhof and R. Zengerle, "Pairs of metallic crosses as a left-handed metamaterial with improved polarization properties," *Opt. Express*, vol. 14, no. 18, pp. 8257–8262, Sep. 2006.
[33] S. Zhang, W. Fan, N. C. Panoiu, K. J. Malloy, R. M. Osgood, and S. R. J. Brueck, "Experimental demonstration of near-infrared negative-index metamaterials," *Phys. Rev. Lett.*, vol. 95, no. 13, pp. 137 404-1–137 404-4, Sep. 2005.
[34] N. Katsarakis, T. Koschny, M. Kafesaki, E. N. Economou, and C. M. Soukoulis, "Electric coupling to the magnetic resonance of split ring resonators," *Appl. Phys. Lett.*, vol. 84, no. 15, pp. 2943–2945, Apr. 2004.
[35] R. Marqués, F. Medina, and R. Rafii-El-Idrissi, "Role of bianisotropy in negative permeability and left-handed metamaterials," *Phys. Rev. B, Condens. Matter*, vol. 65, no. 14, pp. 144 440-1–144 440-6, Apr. 2002.
[36] V. G. Veselago, "The electrodynamics of substances with simultaneously negative values of ϵ and μ," *Sov. Phys.—Usp.*, vol. 10, no. 4, pp. 509–514, 1968.
[37] R. Marqués and D. R. Smith, "Comment on 'Electrodynamics of metallic photonic crystals and the problem of left-handed materials'," *Phys. Rev. Lett.*, vol. 92, no. 5, p. 059401, Feb. 2004.
[38] M. Bayindir, K. Aydin, E. Ozbay, P. Markoš, and C. M. Soukoulis, "Transmission properties of composite metamaterials in free space," *Appl. Phys. Lett.*, vol. 81, no. 1, pp. 120–122, Jul. 2002.
[39] I. V. Shadrivov, D. A. Powell, S. K. Morrison, Y. S. Kivshar, and G. N. Milford, "Scattering of electromagnetic waves in metamaterial superlattices," *Appl. Phys. Lett.*, vol. 90, no. 20, pp. 201 919-1–201 919-3, May 2007.

[40] T. Weiland, R. Schuhmann, R. B. Greegor, C. G. Parazzoli, A. M. Vetter, D. R. Smith, D. C. Vier, and S. Schultz, "*Ab initio* numerical simulation of left-handed metamaterials: Comparison of calculations and experiments," *J. Appl. Phys.*, vol. 90, no. 10, pp. 5419–5424, Nov. 2001.
[41] T. A. Klar, A. V. Kildishev, V. P. Drachev, and V. M. Shalaev, "Negative-index metamaterials: Going optical," *IEEE J. Sel. Topics Quantum Electron.*, vol. 12, no. 6, pp. 1106–1115, Nov./Dec. 2006.
[42] J. Valentine, S. Zhang, T. Zentgraf, E. Ulin-Avila, D. A. Genov, G. Bartal, and X. Zhang, "Three-dimensional optical metamaterial with a negative refractive index," *Nature*, vol. 455, no. 7211, pp. 376–379, Sep. 2008.
[43] N. Liu, H. Guo, L. Fu, S. Kaiser, H. Schweizer, and H. Giessen, "Three-dimensional photonic metamaterials at optical frequencies," *Nat. Mater.*, vol. 7, no. 1, pp. 31–37, Jan. 2008.
[44] A. Ishikawa, T. Tanaka, and S. Kawata, "Negative magnetic permeability in the visible light region," *Phys. Rev. Lett.*, vol. 95, no. 23, pp. 237 401-1–237 401-4, Dec. 2005.
[45] D. Abbott and X.-C. Zhang, "Scanning the issue: T-ray imaging, sensing, and retection," *Proc. IEEE*, vol. 95, no. 8, pp. 1509–1513, Aug. 2007.
[46] W. Withayachumnankul, G. M. Png, X. X. Yin, S. Atakaramians, I. Jones, H. Lin, B. S. Y. Ung, J. Balakrishnan, B. W.-H. Ng, B. Ferguson, S. P. Mickan, B. M. Fischer, and D. Abbott, "T-ray sensing and imaging," *Proc. IEEE*, vol. 95, no. 8, pp. 1528–1558, Aug. 2007.
[47] B. Ferguson and X.-C. Zhang, "Materials for terahertz science and technology," *Nat. Mater.*, vol. 1, no. 1, pp. 26–33, 2002.
[48] M. van Exter, C. Fattinger, and D. Grischkowsky, "High-brightness terahertz beams characterized with an ultrafast detector," *Appl. Phys. Lett.*, vol. 55, no. 4, pp. 337–339, Jul. 1989.
[49] D. M. Mittleman, R. H. Jacobsen, and M. C. Nuss, "T-ray imaging," *IEEE J. Sel. Topics Quantum Electron.*, vol. 2, no. 3, pp. 679–692, Sep. 1996.
[50] F. Huang, B. Schulkin, H. Altan, J. F. Federici, D. Gary, R. Barat, D. Zimdars, M. Chen, and D. B. Tanner, "Terahertz study of 1, 3, 5-trinitro-s-triazine by time-domain and Fourier transform infrared spectroscopy," *Appl. Phys. Lett.*, vol. 85, no. 23, pp. 5535–5537, Dec. 2004.
[51] B. M. Fischer, M. Hoffmann, H. Helm, G. Modjesch, and P. U. Jepsen, "Chemical recognition in terahertz time-domain spectroscopy and imaging," *Semicond. Sci. Technol.*, vol. 20, no. 7, pp. S246–S253, Jul. 2005.
[52] B. Ferguson, S. Wang, D. Abbott, and X.-C. Zhang, "Powder retection with THz imaging," in *Proc. SPIE—Terahertz for Military and Security Applications*, 2003, vol. 5070, pp. 7–16.
[53] P. R. Coward and R. Appleby, "Development of an illumination chamber for indoor millimeter-wave imaging," in *Proc. SPIE—Passive Millimeter-Wave Imaging Technology VI and Radar Sensor Technology VII*, 2003, vol. 5077, pp. 54–61.
[54] C. Zandonella, "T-ray specs," *Nature*, vol. 424, no. 6950, pp. 721–722, Aug. 2003.
[55] D. R. Smith, J. B. Pendry, and M. C. K. Wiltshire, "Metamaterials and negative refractive index," *Science*, vol. 305, no. 5685, pp. 788–792, Aug. 2004.
[56] R. B. Greegor, C. G. Parazzoli, K. Li, and M. H. Tanielian, "Origin of dissipative losses in negative index of refraction materials," *Appl. Phys. Lett.*, vol. 82, no. 14, pp. 2356–2358, Apr. 2003.
[57] H. O. Moser, B. D. F. Casse, O. Wilhelmi, and B. T. Saw, "Terahertz response of a microfabricated rod–split-ring-resonator electromagnetic metamaterial," *Phys. Rev. Lett.*, vol. 94, no. 6, pp. 063901-1–063901-4, Feb. 2005.
[58] H. Tao, A. C. Strikwerda, K. Fan, C. M. Bingham, W. J. Padilla, X. Zhang, and R. D. Averitt, "Terahertz metamaterials on free-standing highly-flexible polyimide substrates," *J. Phys. D, Appl. Phys.*, vol. 41, no. 23, pp. 232 004-1–232 004-5, Dec. 2008.
[59] T. F. Gundogdu, I. Tsiapa, A. Kostopoulos, G. Konstantinidis, N. Katsarakis, R. S. Penciu, M. Kafesaki, E. N. Economou, T. Koschny, and C. M. Soukoulis, "Experimental demonstration of negative magnetic permeability in the far-infrared frequency regime," *Appl. Phys. Lett.*, vol. 89, no. 8, pp. 084103-1–084103-3, Aug. 2006.
[60] M. Aznabet, M. Navarro-Cia, S. A. Kuznetsov, A. V. Gelfand, N. I. Fedorinina, Y. G. Goncharov, M. Beruete, O. E. Mrabet, and M. Sorolla, "Polypropylene-substrate-based SRR- and CSRR-metasurfaces for submillimeter waves," *Opt. Express*, vol. 16, no. 22, pp. 18 312–18 319, Oct. 2008.
[61] H.-T. Chen, W. J. Padilla, J. M. O. Zide, A. C. Gossard, A. J. Taylor, and R. D. Averitt, "Active terahertz metamaterial devices," *Nature*, vol. 444, no. 7119, pp. 597–600, Nov. 2006.
[62] H.-T. Chen, J. F. O'Hara, A. K. Azad, A. J. Taylor, R. D. Averitt, D. B. Shrekenhamer, and W. J. Padilla, "Experimental demonstration of frequency-agile terahertz metamaterials," *Nat. Photon.*, vol. 2, pp. 295–298, 2008.
[63] T. J. Yen, W. J. Padilla, N. Fang, D. C. Vier, D. R. Smith, J. B. Pendry, D. N. Basov, and X. Zhang, "Terahertz magnetic response from artificial materials," *Science*, vol. 303, no. 5663, pp. 1494–1496, Mar. 2004.
[64] T. Driscoll, G. O. Andreev, D. N. Basov, S. Palit, S. Y. Cho, N. M. Jokerst, and D. R. Smith, "Tuned permeability in terahertz split-ring resonators for devices and sensors," *Appl. Phys. Lett.*, vol. 91, no. 6, pp. 062511-1–062511-3, Aug. 2007.
[65] M. Gokkavas, K. Guven, I. Bulu, K. Aydin, R. S. Penciu, M. Kafesaki, C. M. Soukoulis, and E. Ozbay, "Experimental demonstration of a left-handed metamaterial operating at 100 GHz," *Phys. Rev. B, Condens. Matter*, vol. 73, no. 19, pp. 193 103-1–193 103-4, May 2006.
[66] B. D. F. Casse, H. O. Moser, J. W. Lee, M. Bahou, S. Inglis, and L. K. Jian, "Towards three-dimensional and multilayer rod-split-ring metamaterial structures by means of deep X-ray lithography," *Appl. Phys. Lett.*, vol. 90, no. 25, pp. 254 106-1–254 106-3, Jun. 2007.
[67] O. Paul, C. Imhof, B. Reinhard, R. Zengerle, and R. Beigang, "Negative index bulk metamaterial at terahertz frequencies," *Opt. Express*, vol. 16, no. 9, pp. 6736–6744, Apr. 2008.
[68] V. M. Shalaev, "Transforming light," *Science*, vol. 322, no. 5900, pp. 384–386, Oct. 2008.
[69] R. A. Shelby, D. R. Smith, and S. Schultz, "Experimental verification of a negative index of refraction," *Science*, vol. 292, no. 5514, pp. 77–79, Apr. 2001.
[70] P. Gay-Balmaz and O. J. F. Martin, "Efficient isotropic magnetic resonators," *Appl. Phys. Lett.*, vol. 81, no. 5, pp. 939–941, Jul. 2002.
[71] H. O. Moser, J. A. Kong, L. K. Jian, H. S. Chen, G. Liu, M. Bahou, S. M. P. Kalaiselvi, S. M. Maniam, X. X. Cheng, B. I. Wu, P. D. Gu, A. Chen, S. P. Heussler, S. bin Mahmood, and L. Wen, "Free-standing THz electromagnetic metamaterials," *Opt. Express*, vol. 16, no. 18, pp. 13 773–13 780, Sep. 2008.

[72] D. Wu, N. Fang, C. Sun, X. Zhang, W. J. Padilla, D. N. Basov, D. R. Smith, and S. Schultz, "Terahertz plasmonic high pass filter," *Appl. Phys. Lett.*, vol. 83, no. 1, pp. 201–203, Jul. 2003.
[73] B. D. F. Casse, H. O. Moser, L. K. Jian, M. Bahou, O. Wilhelmi, B. T. Saw, and P. D. Gu, "Fabrication of 2D and 3D electromagnetic metamaterials for the terahertz range," *J. Phys.: Conf. Ser.*, vol. 34, pp. 885–890, 2006.
[74] A. K. Azad, J. Dai, and W. Zhang, "Transmission properties of terahertz pulses through subwavelength double split-ring resonators," *Opt. Lett.*, vol. 31, no. 5, pp. 634–636, Mar. 2006.
[75] R. Singh, C. Rockstuhl, F. Lederer, and W. Zhang, "The impact of nearest neighbor interaction on the resonances in terahertz metamaterials," *Appl. Phys. Lett.*, vol. 94, no. 2, pp. 021116-1–021116-3, Jan. 2009.
[76] R. Singh, E. Smirnova, A. J. Taylor, J. F. O'Hara, and W. Zhang, "Optically thin terahertz metamaterials," *Opt. Express*, vol. 16, no. 9, pp. 6537–6543, Apr. 2008.
[77] J. F. O'Hara, E. Smirnova, A. K. Azad, H.-T. Chen, and A. J. Taylor, "Effects of microstructure variations on macroscopic terahertz metafilm properties," *Act. Passive Electron. Compon.*, vol. 2007, pp. 49 691-1–49 691-10, 2007.
[78] A. K. Azad, A. J. Taylor, E. Smirnova, and J. F. O'Hara, "Characterization and analysis of terahertz metamaterials based on rectangular split-ring resonators," *Appl. Phys. Lett.*, vol. 92, no. 1, pp. 011 119-1–011 119-3, Jan. 2008.
[79] H.-T. Chen, J. F. O'Hara, A. J. Taylor, R. D. Averitt, C. Highstrete, M. Lee, and W. J. Padilla, "Complementary planar terahertz metamaterials," *Opt. Express*, vol. 15, no. 3, pp. 1084–1095, Feb. 2007.
[80] J. F. O'Hara, E. Smirnova, H.-T. Chen, A. J. Taylor, R. D. Averitt, C. Highstrete, M. Lee, and W. J. Padilla, "Properties of planar electric metamaterials for novel terahertz applications," *J. Nanoelectronics Optoelectron.*, vol. 2, no. 1, pp. 90–95, Apr. 2007.
[81] N. Katsarakis, G. Konstantinidis, A. Kostopoulos, R. S. Penciu, T. F. Gundogdu, M. Kafesaki, E. N. Economou, T. Koschny, and C. M. Soukoulis, "Magnetic response of split-ring resonators in the far-infrared frequency regime," *Opt. Lett.*, vol. 30, no. 11, pp. 1348–1350, Jun. 2005.
[82] T. Driscoll, G. O. Andreev, D. N. Basov, S. Palit, T. Ren, J. Mock, S.-Y. Cho, N. M. Jokerst, and D. R. Smith, "Quantitative investigation of a terahertz artificial magnetic resonance using oblique angle spectroscopy," *Appl. Phys. Lett.*, vol. 90, no. 9, pp. 092508-1–092508-3, Mar. 2007.
[83] C. Imhof and R. Zengerle, "Strong birefringence in left-handed metallic metamaterials," *Opt. Commun.*, vol. 280, no. 1, pp. 213–216, Dec. 2007.
[84] J. B. Pendry, "A chiral route to negative refraction," *Science*, vol. 306, no. 5700, pp. 1353–1355, Nov. 2004.
[85] S. Zhang, Y.-S. Park, J. Li, X. Lu, W. Zhang, and X. Zhang, "Negative refractive index in chiral metamaterials," *Phys. Rev. Lett.*, vol. 102, no. 2, pp. 023901-1–023901-4, Jan. 2009.
[86] A. Bitzer, H. Merbold, A. Thoman, T. Feurer, H. Helm, and M. Walther, "Terahertz near-field imaging of electric and magnetic resonances of a planar metamaterial," *Opt. Express*, vol. 17, no. 5, pp. 3826–3834, Mar. 2009.
[87] G. Acuna, S. F. Heucke, F. Kuchler, H. T. Chen, A. J. Taylor, and R. Kersting, "Surface plasmons in terahertz metamaterials," *Opt. Express*, vol. 16, no. 23, pp. 18 745–18 751, Nov. 2008.
[88] Y. Yuan, C. Bingham, T. Tyler, S. Palit, T. H. Hand, W. J. Padilla, D. R. Smith, N. M. Jokerst, and S. A. Cummer, "Dual-band planar electric metamaterial in the terahertz regime," *Opt. Express*, vol. 16, no. 13, pp. 9746–9752, Jun. 2008.
[89] C. M. Bingham, H. Tao, X. Liu, R. D. Averitt, X. Zhang, and W. J. Padilla, "Planar wallpaper group metamaterials for novel terahertz applications," *Opt. Express*, vol. 16, no. 23, pp. 18 565–18 575, Nov. 2008.
[90] F. Miyamaru, Y. Saito, M. W. Takeda, B. Hou, L. Liu, W. Wen, and P. Sheng, "Terahertz electric response of fractal metamaterial structures," *Phys. Rev. B, Condens. Matter*, vol. 77, no. 4, pp. 045124-1–045124-6, Jan. 2008.
[91] K. Aydin and E. Ozbay, "Capacitor-loaded split ring resonators as tunable metamaterial components," *J. Appl. Phys.*, vol. 101, no. 2, pp. 024911-1–024911-5, Jan. 2007.
[92] Y. Sun, X. Xia, H. Feng, H. Yang, C. Gu, and L. Wang, "Modulated terahertz responses of split ring resonators by nanometer thick liquid layers," *Appl. Phys. Lett.*, vol. 92, no. 22, pp. 221 101-1–221 101-3, Jan. 2008.
[93] I. Gil, J. García-García, J. Bonache, F. Martín, M. Sorolla, and R. Marqués, "Varactor-loaded split ring resonators for tunable notch filters at microwave frequencies," *Electron. Lett.*, vol. 40, no. 21, pp. 1347–1348, Oct. 2004.
[94] I. Gil, J. Bonache, J. García-García, and F. Martín, "Tunable metamaterial transmission lines based on varactor-loaded split-ring resonators," *IEEE Trans. Microw. Theory Tech.*, vol. 54, no. 6, pp. 2665–2674, Jun. 2006.
[95] I. V. Shadrivov, S. K. Morrison, and Y. S. Kivshar, "Tunable split-ring resonators for nonlinear negative-index metamaterials," *Opt. Express*, vol. 14, no. 20, pp. 9344–9349, Oct. 2006.
[96] Q. Zhao, L. Kang, B. Du, B. Li, J. Zhou, H. Tang, X. Liang, and B. Zhang, "Electrically tunable negative permeability metamaterials based on nematic liquid crystals," *Appl. Phys. Lett.*, vol. 90, no. 1, pp. 011112-1–011112-3, Jan. 2007.
[97] X. Wang, D.-H. Kwon, D. H. Werner, I.-C. Khoo, A. V. Kildishev, and V. M. Shalaev, "Tunable optical negative-index metamaterials employing anisotropic liquid crystals," *Appl. Phys. Lett.*, vol. 91, no. 14, pp. 143 122-1–143 122-3, Oct. 2007.
[98] A. A. Zharov, I. V. Shadrivov, and Y. S. Kivshar, "Suppression of left-handed properties in disordered metamaterials," *J. Appl. Phys.*, vol. 97, no. 11, pp. 113 906-1–113 906-3, Jun. 2005.
[99] M. V. Gorkunov, S. A. Gredeskul, I. V. Shadrivov, and Y. S. Kivshar, "Effect of microscopic disorder on magnetic properties of metamaterials," *Phys. Rev. E, Stat. Phys. Plasmas Fluids Relat. Interdiscip. Top.*, vol. 73, no. 5, pp. 056 605-1–056 605-8, May 2006.
[100] J. Han, A. Lakhtakia, and C.-W. Qiu, "Terahertz metamaterials with semiconductor split-ring resonators for magnetostatic tunability," *Opt. Express*, vol. 16, no. 19, pp. 14 390–14 396, Sep. 2008.
[101] H. Tao, N. I. Landy, C. M. Bingham, X. Zhang, R. D. Averitt, and W. J. Padilla, "A metamaterial absorber for the terahertz regime: Design, fabrication and characterization," *Opt. Express*, vol. 16, no. 10, pp. 7181–7188, May 2008.
[102] A. C. Strikwerda, K. Fan, H. Tao, D. V. Pilon, X. Zhang, and R. D. Averitt, "Comparison of birefringent electric split-ring resonator and meanderline structures as quarter-wave plates at terahertz frequencies," *Opt. Express*, vol. 17, no. 1, pp. 136–149, Jan. 2009.
[103] L. Young, L. A. Robinson, and C. A. Hacking, "Meander-line polarizer," *IEEE Trans. Antennas Propag.*, vol. AP-21, no. 3, pp. 376–378, May 1973.
[104] W. J. Padilla, A. J. Taylor, C. Highstrete, M. Lee, and R. D. Averitt, "Dynamical electric and magnetic metamaterial response at terahertz frequencies," *Phys. Rev. Lett.*, vol. 96, no. 10, pp. 107 401-1–107 401-4, Mar. 2006.

[105] H.-T. Chen, W. J. Padilla, J. M. O. Zide, S. R. Bank, A. C. Gossard, A. J. Taylor, and R. D. Averitt, "Ultrafast optical switching of terahertz metamaterials fabricated on ErAs/GaAs nanoisland superlattices," *Opt. Lett.*, vol. 32, no. 12, pp. 1620–1622, Jun. 2007.
[106] H.-T. Chen, S. Palit, T. Tyler, C. M. Bingham, J. M. O. Zide, J. F. O'Hara, D. R. Smith, A. C. Gossard, R. D. Averitt, W. J. Padilla, N. M. Jokerst, and A. J. Taylor, "Hybrid metamaterials enable fast electrical modulation of freely propagating terahertz waves," *Appl. Phys. Lett.*, vol. 93, no. 9, pp. 091 117-1–091 117-3, Sep. 2008.
[107] H.-T. Chen, W. J. Padilla, M. J. Cich, A. K. Azad, R. D. Averitt, and A. J. Taylor, "A metamaterial solid-state terahertz phase modulator," *Nat. Photon.*, vol. 3, pp. 148–151, 2009.
[108] R. Piesiewicz, T. Kleine-Ostmann, N. Krumbholz, D. Mittleman, M. Koch, J. Schoebel, and T. Kurner, "Short-range ultra-broadband terahertz communications: Concepts and perspectives," *IEEE Antennas Propag. Mag.*, vol. 49, no. 6, pp. 24–39, Dec. 2007.
[109] J. T. Kindt and C. A. Schmuttenmaer, "Far-infrared dielectric properties of polar liquids probed by femtosecond terahertz pulse spectroscopy," *J. Phys. Chem.*, vol. 100, no. 24, pp. 10 373–10 379, 1996.
[110] D. M. Mittleman, R. H. Jacobsen, R. Neelamani, R. G. Baraniuk, and M. C. Nuss, "Gas sensing using terahertz time-domain spectroscopy," *Appl. Phys. B, Lasers Opt.*, vol. 67, no. 3, pp. 379–390, Sep. 1998.
[111] I. A. I. Al-Naib, C. Jansen, and M. Koch, "Thin-film sensing with planar asymmetric metamaterial resonators," *Appl. Phys. Lett.*, vol. 93, no. 8, pp. 083 507-1–083 507-3, Aug. 2008.
[112] M. C. K. Wiltshire, J. B. Pendry, and J. V. Hajnal, "Sub-wavelength imaging at radio frequency," *J. Phys., Condens. Matter*, vol. 18, no. 22, pp. L315–L321, Jun. 2006.
[113] A. Grbic and G. Eleftheriades, "Overcoming the diffraction limit with a planar left-handed transmission-line lens," *Phys. Rev. Lett.*, vol. 92, no. 11, pp. 117 403-1–117 403-4, Mar. 2004.
[114] A. N. Lagarkov and V. N. Kissel, "Near-perfect imaging in a focusing system based on a left-handed-material plate," *Phys. Rev. Lett.*, vol. 92, no. 7, pp. 077401-1–077401-4, Feb. 2004.
[115] B.-I. Popa and S. A. Cummer, "Direct measurement of evanescent wave enhancement inside passive metamaterials," *Phys. Rev. E, Stat. Phys. Plasmas Fluids Relat. Interdiscip. Top.*, vol. 73, no. 1, pp. 016617-1–016617-5, Jan. 2006.
[116] N. Fang, H. Lee, C. Sun, and X. Zhang, "Sub-diffraction-limited optical imaging with a silver superlens," *Science*, vol. 308, no. 5721, pp. 534–537, Apr. 2005.
[117] I. I. Smolyaninov, Y.-J. Hung, and C. C. Davis, "Magnifying superlens in the visible frequency range," *Science*, vol. 315, no. 5819, pp. 1699–1701, Mar. 2007.